AIAA JOURNAL
Vol. 31, No. 3, March 1993

Laser Absorption Measurements of OH Concentration and Temperature in Pulsed Facilities

John A. Cavolowsky* and Mark E. Newfield*
NASA Ames Research Center, Moffett Field, California 94035
and
Mark P. Loomis*
MCAT Institute, San Jose, California 95127

A laser absorption flow diagnostic application has been developed at the NASA Ames 16-in. shock tunnel for purposes of measuring the thermochemical state of OH in flow environments of interest. Research objectives include the investigation of high-temperature, low-pressure chemistry pertinent to scramjet combustors and high altitude flight. The system can be operated in either the fixed frequency mode or in the rapid wavelength scanning mode to measure species mole fraction and temperature. Emission diagnostics have been employed to determine shock tunnel flow quality and assist in the proper application of the diagnostic and its data interpretation. Rotational lines in the OH $A^2\Sigma^+ - X^2\Pi$ (0,0) system were probed in the expanding facility nozzle flow and time-resolved measurements of temperature and mole fraction are provided. Facility test time was also measured using this technique. Discussion of diagnostic and operational uncertainties is included.

Introduction

PRIOR to the National Aerospace Plane Technology Maturation Program, there were no ground-based hypersonic flight simulation facilities with instrumentation systems that could provide conditions for proper measurement of fluid mechanical properties and finite rate chemistry in combusting and expanding scramjet combustor flows. Operational facilities existed that could provide certain simulation capabilities, however, with compromises in flight equivalent enthalpy, tunnel test time, test article scale, or diagnostic instrumentation. The 16-in. shock tunnel at the Ames Hypervelocity Free-Flight Aerodynamic Facility (HFFAF) had demonstrated the ability to simulate the necessary velocities and enthalpies with test times longer than other functioning facilities and provide a test section large enough to house nearly full-scale combustor modules.[1-5] The facility, however, had been deactivated 17 years earlier, and its capabilities could not be confirmed.

The only flow diagnostic instrumentation available and understood for use in impulse facilities were surface mounted gauges for measuring pressure and heat transfer at the wall of the test article or the facility. It was clear that proper application of these facilities to scramjet combustors would require a new generation of surface measurement instruments as well as nonintrusive optical diagnostic instruments for measurement of flowfield properties and combustor performance.[6,7] Although laser-based optical diagnostic research is a rapidly maturing field and has shown great promise for its application, the techniques had not been validated in large hypersonic facility test environments. This is, in part, due to the inherent difficulty in developing high-fidelity instruments for use in environments unaccommodating to laser systems. Among the problems in large-scale impulse facilities facing the optical diagnostician are flowfield contaminants, test room thermal gradients, remote laser locations requiring long beam path lengths, relatively short test times (on the order of milliseconds), and long facility turnaround time (nominally one day). As will be described, a major thrust of this work has been the development effort required to make meaningful laser spectroscopic measurements in the Ames 16-in. shock tunnel.

The proposed research objective for the Ames 16-in. shock tunnel involves the investigation of high-temperature, low-pressure chemistry pertinent to scramjet combustor conditions and high altitude flight. This will include the testing of scale models of scramjet injectors and combustion chamber geometries. Implementation of these objectives has begun with the application of a laser absorption system to measure OH concentration and temperature in the expanding flow of the facility nozzle using rapid wavelength scanning techniques. OH was chosen as the species of interest due to its importance in H_2-air combustion chemistry. This laser absorption technique was chosen for several reasons. Primarily, it is a quantitative measurement technique. Although it is a line-of-sight method, laser absorption is a pragmatic choice for applications where optical access is limited. Small windows (as small as several millimeters aperture), sufficient to transmit the beam, can easily be incorporated into most any region of a scramjet engine. The rapid scanning capability of the laser system allows measurements to be made at frequencies of up to 4 kHz covering a wavelength region inclusive of two rotational transitions in OH. This provides for many measurements of OH concentration and rotational temperature during the test period. Although laser absorption is not spatially resolved as are the laser induced fluorescence and coherent anti-Stokes raman spectroscopic techniques, its time-resolved nature eliminates the need for as many repeat tests to achieve adequate statistical significance. Given the inherently short test time and long turnaround time for pulsed facilities, rapid wavelength scanning proves to be a powerful capability.

Experimental Facility

The 16-in. shock tunnel was initially designed to provide high-speed counter flow to a small-scale model launched at hypervelocities from a light-gas gun. This facility system forms what is called the Hypersonic Free-Flight Aerodynamic Facility. A schematic of the shock tunnel portion of the facility is presented in Fig. 1. The 16-in. shock tunnel earns its name from the 16-in. naval cannons that comprise the driver section of the shock tube. The shock tunnel, currently operated inde-

Received March 28, 1992; revision received Aug. 10, 1992; accepted for publication Aug. 12, 1992.

*Research Scientist. Member AIAA.

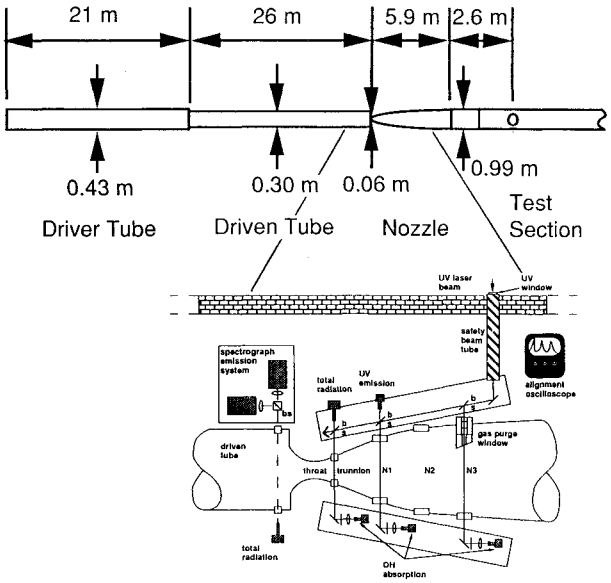

Fig. 1 Schematic of the Ames 16-in. shock tunnel and optical instrumentation in the nozzle section (not to scale).

pendently of the light-gas gun, consists of a 21-m-long × 0.43-m-diam driver tube and a 26-m-long × 0.30-m-diam driven tube with a 5.9-m-long ($M = 7$) nozzle section. For the present results, the nozzle is operated at an area ratio (A/A^*) of 271. Copper or steel nozzle throat inserts with a throat diameter of 6 cm are used. The range of facility operation conditions is published in the open literature.[8]

All diagnostic measurements are made at the same flow conditions. The driver gas is combustion heated helium at a peak pressure of 6.89 MPa. This is generated by burning a mixture of hydrogen/oxygen/helium in proportions of 3/1/8. The primary diaphragm is 1.6-mm-thick stainless steel and is ruptured either by means of an explosive tape or an explosively driven lance. The driven tube is maintained at a pressure of 8.7 kPa and is separated from the nozzle and test section by the nozzle diaphragm, a thin sheet of either Mylar† or aluminum. Test section pressure prior to the flow was maintained at 0.013 kPa. The driven gas to driver gas (pre-burn) pressure ratio is 0.010.

The incident shock speed is 3.0 km/s, varying somewhat with the driver gas mixture and pressure level. The nozzle reservoir conditions are those behind the reflected shock at the end of the driven tube. This shock speed generates a nozzle reservoir enthalpy of about 9500 J/g, a temperature of about 5700 K, and a pressure of about 6.2 MPa. The pressure is a measured quantity whereas the enthalpy and temperature are calculated using standard shock tube relations. The test time, based only on the arrival of the reflected driver expansion wave, is 0.017 s (see Fig. 2). Actual driver gas free test times are expected to be considerably shorter (typically by factors of 2–4).

Optical access is provided at four nozzle locations shown in expanded view portion of Fig. 1: the trunnion (Tr), nozzle location 1 (N1), nozzle location 2 (N2), and nozzle location 3 (N3). The test measurement location used for this work is N1 which has an area ratio of 73 and a line-of-sight path length diametrically across the nozzle of 51.5 cm. A 23-m-long, 1.0-m-diam test section and associated dump tank is located downstream of the nozzle.

Optical Instrumentation

The laser system used in the initial shock tunnel investigations is shown in Fig 3. This system has been developed by Hanson and associates at the High Temperature Gasdynamics Laboratory at Stanford University and is described in detail in Refs. 9 and 10. A brief description of the basic system and its specific application in the 16-in. shock tunnel will follow. A remotely located continuous wave argon ion pumped ring dye laser (Spectra-Physics Model 380C) with temperature tuned intracavity second harmonic generation in deuterated ammonium dihydrogen arsenate (AD*A) was used in the ultraviolet near 306 nm. The laser dye is Rhodamine 590. This system provides a wavelength operation range of 295–307 nm limited by the AD*A crystal. The typical uv power level is 5–10 mW, and the laser has an effective spectral line width of approximately 1 MHz. Scanning over a narrow wavelength region is accomplished with an intracavity dual rhomb oscillator operated at frequencies up to 4 kHz. The power meter and the wave meter located in the visible beam path monitor laser intensity and wavelength, and the fixed 2.00-GHz visible etalon provides a frequency marker as the laser is scanned in wavelength. A reference uv beam intensity measurement is made prior to beam passage through the test section, and a similar photodiode detector, located at the nozzle, measures the beam intensity after interaction with the test flow. The detectors have a roll-off frequency of no less than 400 kHz. Efforts are made to balance signal levels from the reference detector and the postflow interaction detector to reduce error associated with the data reduction process.

The laser system is separated from the shock tunnel by a 47-cm-thick concrete wall. The laser beam is directed through a tube in the wall to an optical rail flanking the nozzle test section. As seen in Fig. 1, the beam is distributed to the individual nozzle windows by a series of mirrors and beam splitters at which point it is sent through the nozzle and collected on filtered detectors mounted on another optical rail flanking the opposite side of the nozzle. Two 1-m focal length lenses are positioned in the beam path prior to the nozzle to reduce beam divergence. The window material is uv grade fused silica and has a viewing aperture diameter of 3.6 cm for nozzle locations N1, N2, and N3. The aperture is limited to 1.3 cm at the trunnion. Smaller windows, 0.5-cm-diam aperture, are also provided at the reflected shock region in the driven tube.

In conjunction with the laser absorption measurements, spectrographic records are acquired at various points in the shock tunnel flow. These records are necessary to assist in the determination of sources of flow contamination detrimental to the laser based measurements. Spectrally resolved emission signatures from the reflected shock region are measured using a 0.75-m ℓ7 Jarrell-Ash spectrograph. Test section emission from core flow gas behind the bow shock at a pitot rake located in the test section downstream of the nozzle exit is measured using a Huet ℓ3.5 prism spectrograph. All spectrographs are independently shuttered. Complimentary emission measurements were made in the driven tube, at the trunnion, and at N1 using coupled monochromator/photomultiplier systems, photoresistive total emission detectors, and photodiode

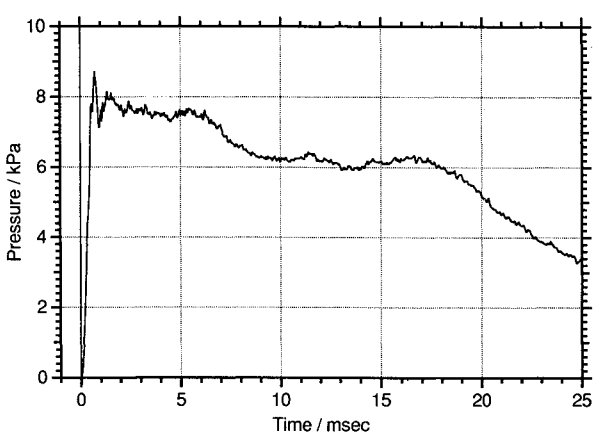

Fig. 2 Nozzle static pressure at nozzle station N1.

†Mention of a specific manufacturer is for identification purposes only and does not imply endorsement by NASA.

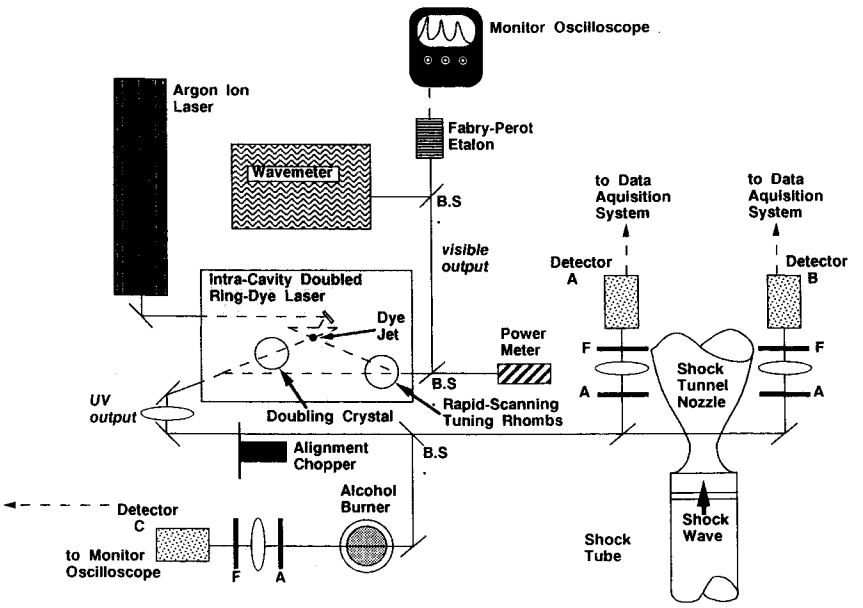

Fig. 3 Laser absorption instrumentation.

detectors filtered for broadband uv emission. Total emission is also measured using broadband United Detector PIN 10D photoconductive detectors at various locations along the shock tunnel for purposes of timing.

The data is collected in the remote laser room using a stand-alone 16-channel modular CAMAC standard data acquisition system by LeCroy. The digitizing modules (Model 6810) have a maximum sampling rate of 1 megasample/s, 512-KB record length, 12-bit vertical resolution, and variable gain. A custom software package[11] using National Instruments Labview interface control software records the raw signal and WaveMetrics Igor software is used for analysis and graphics on an Apple Macintosh IIfx.

Theory

The transmission of a beam of light at a given wavelength passing through an absorbing medium is given by the Beer-Lambert law[12]:

$$I(\nu) = I_0 \exp\int_0^L - k_\nu P_{\text{abs}}\, dx \tag{1}$$

Here I_0 is the intensity of the incident beam, I the intensity of the beam after having passed through the absorbing medium along a path of length L, k_ν the wavelength-dependent absorption coefficient, and P_{abs} the partial pressure of the absorbing species. The absorption coefficient near an isolated spectral line can be described as the product of the integrated line intensity S_{lu} and a line shape function $\phi(\nu)$

$$k_\nu = S_{lu}\phi(\nu) \tag{2}$$

The line intensity S_{lu} is readily calculated from tabulated spectral parameters.[12,13] The Voigt function is the convolution of the Gaussian profile due to Doppler broadening with a Lorentzian profile due to collisional or pressure broadening and has been shown to model the OH absorption line shape function quite well. The Voigt function cannot be evaluated analytically, but algorithms have been established for rapid computation of the function.[14] The proportion of these two components has been defined through the Voigt a parameter

$$a = [\ell n(2)]^{1/2}\Delta\nu_c/\Delta\nu_D \tag{3}$$

where $\Delta\nu_c$ is the collisional linewidth and $\Delta\nu_D$ the Doppler line width. For OH, the Doppler linewidth is given by

$$\Delta\nu_D = 1.7368 \times 10^{-7}\nu_0 T^{1/2} \quad (\text{cm}^{-1}) \tag{4}$$

where the line center ν_0 is in cm^{-1}, and T is in Kelvin. The collisional linewidth must generally be measured over the desired pressure and temperature range of interest.[15] A functional form of

$$a = kP/T_{\text{ref}}(T_{\text{ref}}/T) \tag{5}$$

was used to account for the collisional broadening, with $k = 350$ K/atm and $T_{\text{ref}} = 1600$ K.

The intensity ratio of two lines R, shown to be the ratio of the observed absorption coefficients, can also be expressed as the ratio of Boltzmann fractions

$$R = C_2 \exp(-E_2/kT)/\left[C_1 \exp(-E_1/kT)\right]$$
$$= C \exp(-B/T) \tag{6}$$

Since this temperature dependence in R is due to the exponential behavior of the Boltzmann fraction, it is independent of concentration. It can be shown[12,13] that for OH A-X (0,0) $R_1(11)$ and $R_1(7)$, B is equal to 1995 K and C is equal to 1.508. As will be discussed subsequently, these two rotational transitions are accessible within the tuning region of the AD*A doubling crystal and are closely spaced in frequency so as to lie in the scanning region of the dual rhomb oscillator. Thus the rotational temperature can be determined using the rapid wavelength scanning technique.

At flow conditions of interest, the accessible rotational lines will exhibit linewidths of approximately 10 GHz compared to the very narrow laser line width of 1 MHz. It is, therefore, possible to measure mole fractions using the fixed frequency mode of operation where the laser is carefully tuned to the line center or to measure the full line shape with the scanning option. Mole fraction is determined by Eq. (1) either using the peak height (obtained from fixed frequency or scanning measurements) along with knowledge of the temperature or by integrating the absorption coefficient for a single line shape.

Data Reduction

Figure 4 is a plot of the fractional transmission I/I_0 from a typical run. Figure 5 is an expanded plot showing just two line pairs and the associated etalon trace. If the assumption is made that the thermodynamic conditions and concentration of OH are constant along the path length, then Eq. (1) can be simplified to

$$I(\nu) = I_0 \exp(-k_\nu P_{\text{abs}} L) \tag{7}$$

Although there is no experimental evidence to directly verify this assumption, recent computations[16] indicate that pressure and temperature profiles across the flow at nozzle location N1 vary by approximately less than 5%. The boundary-layer thickness is expected to be small (less than 2 cm) as will be its effect on the measured averaged OH concentration. To test this, 7-cm-long extension tubes were fitted to the N1 window ports to allow only the flow beyond the boundary layer to be probed. No measurable difference in absorption signal was observed between the tests where the extenders were used and where they were not used.

The data is then reduced in the form $-\ell n[I(\nu)/I_0]$ (see Fig. 6 and the comparison to the OH reference source). Since each etalon peak represents a 4-GHz frequency change in the ultraviolet, the time base can be converted to a frequency base by assuming a sinusoidal frequency variation in time. The line profiles are fit with Voigt profiles using the Igor plotting and analysis package. Figure 7 shows the results of Voigt fits to a line pair. Gaussian fits can be used as an approximation of the line shape. This would, however, introduce an error of nearly 4% due to neglect of the Lorentzian broadening contribution. For this study, all line shapes were fit with Voigt profiles.

The rotational temperature is determined by the ratio of the area under each line pair and by using Eq. (6). Translational temperature can be determined from the Doppler linewidth, however, this method requires assumptions about the collisional broadening and is not as accurate as the determination of the rotational temperature (equilibrium is assumed so that the translational temperature is equal to the rotational temperature). Once temperature is determined, the partial pressure or mole fraction of OH is determined using Eqs. (2) and (7) along with known spectroscopic constants, the value of the absorption coefficient at the line center determined from the curve fit analysis, and the measured path length. The 1-MHz spectral line width of the laser does not compromise the precise definition of the rotational line width, nor is the data compromised due to digitizing error or bit noise given the 12-bit vertical resolution and sampling rate of 1 megasample/s available from the digitizing units.

Initial reduction of the data revealed a discrepancy in the two methods used to calculate the temperature. The rotational temperature calculated from Eq. (6) was about 20% lower than what was calculated from the inferred translational temperature using the result of the Voigt fit and Eq. (4). The discrepancy was eliminated by noting that the measurement was made in the expanding part of the shock tunnel nozzle where there was a finite radial velocity. The effect of this radial velocity is to produce a Doppler shift in the local absorption profile. Since the shift is symmetric about the tunnel centerline, the net effect was to cause an effective broadened profile. Calculations show that this effect caused an apparent 9% broadening of the Gaussian line width. Thus the data was reduced with a 9% correction to the inferred Gaussian (or Doppler) line width. With this correction applied, the temperature inferred from both measurements agreed within the experimental uncertainty. Since the broadening also reduced the peak height, a correction was also applied to the OH number density calculated from Eq. (7).

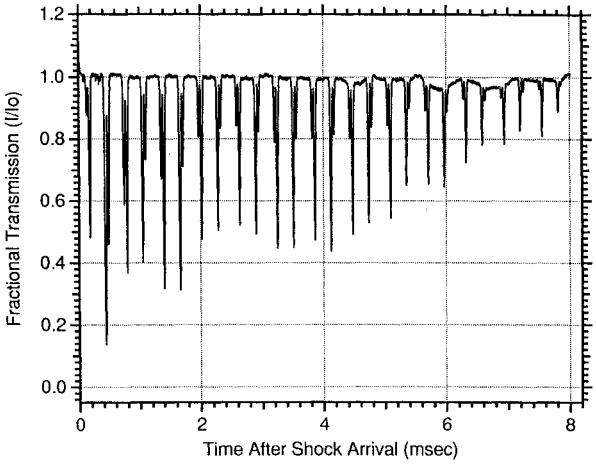

Fig. 4 Wavelength scan of OH A-X(0,0) $R_1(7)$ and $R_1(11)$ at nozzle station N1: test gas is 10% mole fraction of water in nitrogen.

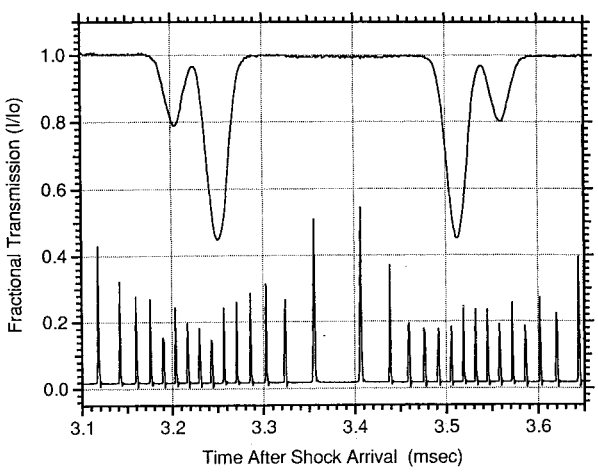

Fig. 5 Expanded wavelength scan showing two line pairs and associated etalon trace.

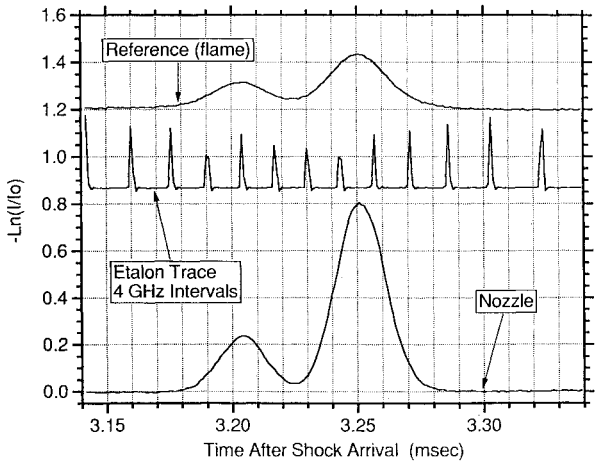

Fig. 6 Reduced data from wavelength scan showing reference flame data.

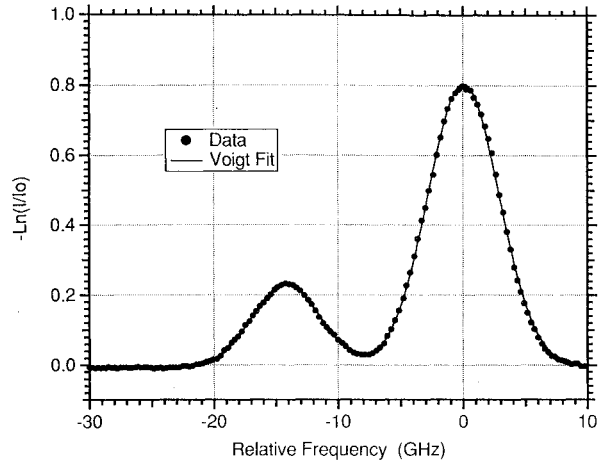

Fig. 7 Reduced data fit to a Voigt profile plotted vs relative spectral frequency.

Diagnostic Application Development

Prior to determination of species concentration and temperature, the nozzle flow quality must be evaluated. This involves determination of the test time of the shock tunnel as defined by the period during which driven gas, uncorrupted by the helium driver gas, passes through the test section. It was determined that the laser system, used in its basic fixed-frequency configuration to detect the presence of OH at one nozzle location, could be used to this end if the driven gas would be saturated with water prior to the test. OH formed upon shock heating of the driven gas would be detected by the absorption laser system. When the OH signal begins to decrease, the driver gas is assumed to have arrived displacing the driven tube test gas; and the uncontaminated test period is complete. A time dependent, nonequilibrium computational model was used to estimate OH concentration and thermodynamic conditions in the driven gases as they expand within the nozzle. The $R_1(5)$ $A^2\Sigma^+ \leftarrow X^2\Pi$ (0,0) line at 306.687 nm was chosen since its variation in absorption coefficient is minimal over the range of temperatures expected in the nozzle.

Transferring this laser absorption technology from the research laboratory to the practical facility proved to be a challenging task. It became evident in the very first series of results that there was significant attenuation of the laser beam by flowfield contaminants as well as emission from the flow that artificially increased the apparent beam transmission. It was necessary therefore to first identify the sources of contamination and eliminate them before meaningful OH absorption measurements could be made. This was accomplished by two means. First, the laser system was tuned to a stable wavelength close to the $R_1(5)$ transition but not at an OH resonant frequency. The contaminants therefore would absorb the off-resonance radiation to essentially the same degree as they would the on-resonance radiation. With this technique, the sources of flow contamination were systematically identified and removed. This is an excellent example of the versatility of this nonintrusive, laser-based flow diagnostic. Second, several methods of emission measurement were implemented as described previously, and the strong emission sources were also identified and removed.

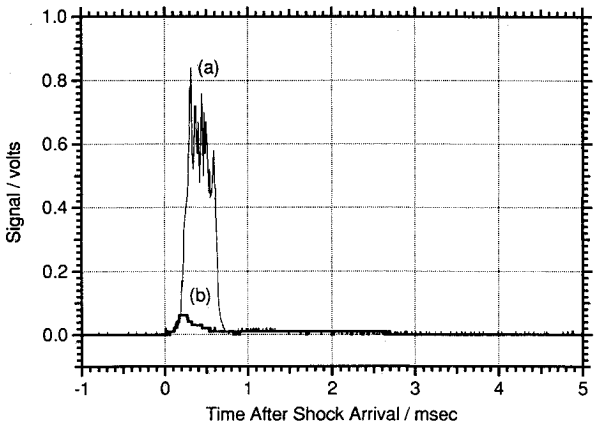

Fig. 8 Ultraviolet emission measurements at nozzle station N1: a) aluminum nozzle diaphragm; high explosive rupture of primary diaphragm and b) Mylar nozzle diaphragm; lance rupture of primary diaphragm.

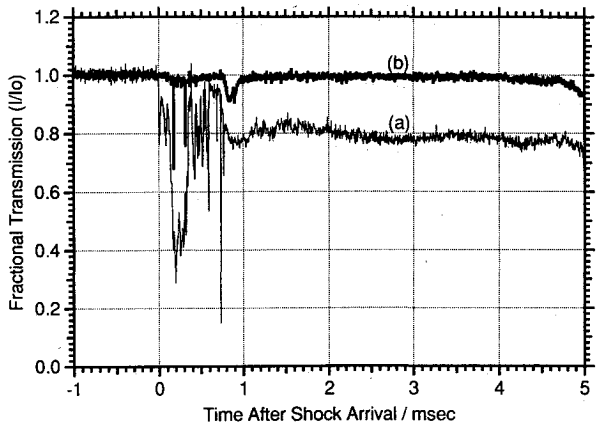

Fig. 9 Offline fractional transmission measurements at nozzle station N1: a) aluminum nozzle diaphragm; high explosive rupture of primary diaphragm and b) Mylar nozzle diaphragm; lance rupture of primary diaphragm.

Many sources of flowfield contamination were discovered and eliminated. The nozzle valve, used to prevent main diaphragm fragments from entering the test section, was found to contribute iron to the core flow and consequently was removed. Both steel and copper nozzle throat inserts were evaluated for their contribution to metal oxides in the flow, and no measurable difference was detected. This is not to imply that different amounts of material was not being removed from the nozzle throats but rather that the difference was not detected by the laser system. The steel nozzle insert was chosen for reasons that will be discussed shortly. Gas bleed window adapters and extension tubes permitting optical access to the flow beyond the boundary layer were installed to help keep deposits off the windows. At the conditions examined in this test program, the gas bleed adapters and extension tubes were eventually determined to be nonessential.

Two particular sources were found to contribute most significantly to contamination levels in the flow: 1) the nozzle diaphragm and 2) the high explosive used to rupture the primary diaphragm.

Two different nozzle diaphragm materials, aluminum and Mylar, were tested and found to effect the laser absorption signal by attenuation and by emission. Aluminum diaphragms were a large source of metal oxide particulates that severely attenuated the uv laser beam and also emitted strongly in the uv artificially increasing intensities (Fig. 8a). It was replaced in favor of Mylar which provided very little emission but did fragment and attenuate the signal as well as contribute OH from its own combustion (Fig. 8b). As the mass of the diaphragm was reduced, however, the attenuation due to the Mylar was also reduced. Ultimately, a 0.025-mm-thick Mylar diaphragm was used. This is a practical minimum thickness to support the pressure differential between the driven tube and the test section. It was for these reasons that the steel nozzle insert, which can mount a smaller diameter nozzle diaphragm, was chosen as the baseline nozzle.

Finally, by eliminating the high explosive tape as the primary diaphragm rupture actuator and replacing it with a prescored diaphragm that is ruptured by an explosively driven lance, the flow was left virtually uncontaminated for a period of over 30 ms after shock arrival (Figs. 9a and 9b). The only remaining signal attenuations occur within the first 2 ms and are small contributions from Mylar combustion products and nozzle diaphragm fragments. This period is coincidentally associated with the unsteady flow portion of the nozzle start up process and is, therefore, conveniently discarded for reasons of flow physics.

OH Measurements Using Fixed Wavelength Technique

Having effectively eliminated the nozzle flowfield contaminants responsible for artificial signal attenuation and augmentation, it was possible to retune the laser to the $R_1(5)$ resonance wavelength and probe the driven gas flow for OH. Figure 10 shows the plot of fractional transmission vs time after shock arrival at the N1 nozzle location for the $R_1(5)$ line. The water vapor mole fraction of the driven tube gas was 10% in nitrogen. Examination of the data shows that immediately after shock arrival (designated time zero) there occurs a sharp increase in OH concentration. This is interpreted to be due to combustion of the Mylar nozzle diaphragm generating OH as an intermediate species. The contribution from the nozzle

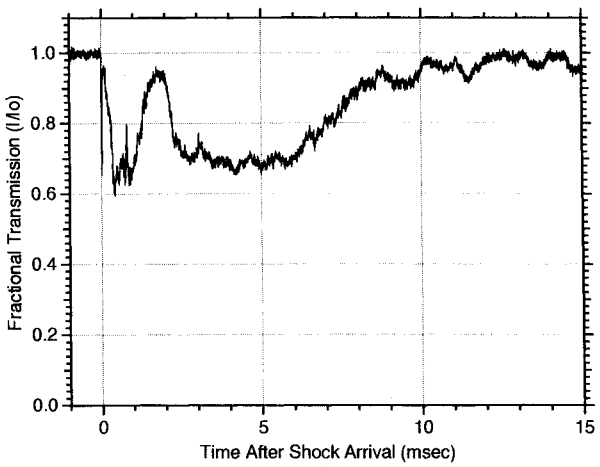

Fig. 10 Fixed wavelength fractional transmission record of OH A-X(0,0) $R_1(5)$ at nozzle station N1: test gas is 23% mole fraction of water in nitrogen.

diaphragm exists for a limited duration of approximately 1.7 ms before it sharply disappears returning to the nearly 100% beam transmission level. Since this time period conveniently coincides with the nonuseful nozzle flow establishment period, the absorption and attenuation in this region can be disregarded. This event is quickly followed by the arrival of OH associated with the driven tube test gas flow. The absorption signal is attenuated by 30% and remains virtually constant for a period of close to 4 ms before it slowly decays over a period of about 5 ms to the near 100% transmission level. This behavior is interpreted as the gradual intrusion of helium from the driver gas present in the diffuse contact surface generated during the primary diaphragm rupture process and from the driven tube boundary layer.

Several tests conducted at this condition produced data indicating a range of useful test time of between 3 and 5 ms. This spread in test time is not unusual in impulse facilities given the inherent variation in primary diaphragm rupture characteristics. It has been argued that a direct measure of helium arrival time rather than an inference of its arrival by the disappearance of a driven gas species is superior. However, a comparison of test time measured by OH absorption with measurements of total emission at the N1 location and nozzle surface static pressure and heat transfer provide independent confirmation of the 3–5-ms test time range and serves to validate the diagnostic technique.

Given the narrow (1-MHz) line width of the laser compared to the rotational spectral feature being probed, the laser can be accurately tuned to the line peak allowing reduction of the measured absorption to OH mole fraction. It is necessary, however, to know the pressure and temperature of the probe volume to determine the mole fraction. Pressure is routinely measured at the nozzle wall, whereas temperature has previously been determined only computationally. Temperature can now be measured with the rapid wavelength scanning technique.

OH Measurements Using the Rapid Wavelength Scanning Technique

Rapid wavelength scanning over spectrally adjacent absorption lines gives information about species concentration and temperature. This diagnostic, with its high scanning rates, is particularly valuable in large-scale impulse facilities where test times are short and test frequency low. For the nearly 5-ms test period available in a single run of the 16-in. shock tunnel, over 10 independent measures of OH absorption can be made. This greatly reduces the need for large numbers of repeat facility runs to obtain proper measurement statistics.

However, certain considerations must be made before choosing the specific absorption lines. First, it is recognized that the full spectral width of the scan is about two wave numbers. Given this limitation, two adjacent absorption lines within the doubling range of the crystal are chosen that are distinct but separated by no more than one wave number. These chosen lines must have suitably different initial rotational levels such that their Boltzmann fractions are large enough to provide sensitivity to temperature. Since the doubling range of the AD*A crystal is 295–307 nm, only a portion of the lines in the OH A-X (0,0) R branch are available in the scan. Once the lines are chosen and the data acquired, the data are reduced to yield the change in transmission fraction $\Delta I/I_0$. As previously described, the ratio of the transmission fraction peaks is used to extract temperature, and the transmission magnitudes themselves are an indication of the OH mole fraction levels. It was determined that, for this flow environment, temperature and mole fraction of OH can be well measured by a scan including the $R_1(7)$ and $R_1(11)$ transitions.

The technique was evaluated in three data runs made at the same conditions as described earlier. The driven tube gas, however, was water saturated nitrogen at 23% mole fraction.

Re-examining the scanning fractional transmission vs time after shock arrival traces displayed in Fig. 4, one can see the same data features as described for the fixed wavelength data. The peak heights define the magnitude of the absorption to be compared to the fixed wavelength traces. In Fig. 5 the $R_1(7)$ line is the higher of the two peaks of the doublet with the order of the lines alternating as the laser is tuned back and forth in time. The nozzle flow establishment period is followed by the viable test time before driver contamination gradually appears.

Reduction of this data yields an average rotational temperature of 1170 K at nozzle station N1 with a variation of approximately 5% over the test period (Fig. 11a). The significantly higher temperature in the first 1.7 ms is attributed to exothermic energy release of the burning of the thin Mylar diaphragm coupled with contamination augmentation of the absorption signal and is to be ignored. Temperature is not mole fraction dependent, therefore, the peak height variations across the scan do not result in equivalent variations in temperature. Reference 10 reports error bounds of less than ±3% for the diagnostic as applied to high-fidelity shock tube conditions at temperatures near 1200 K. In this study, due to the counteracting effects of enhanced data acquisition system capabilities and flow parameter uncertainties (i.e., boundary-layer effects, nonuniformities, and other two-dimensional concerns), error bounds are difficult to accurately assess. Time-accurate, two-dimensional computational fluid dynamics calculations of the nozzle flow would provide a better understanding of flow parameter uncertainties.

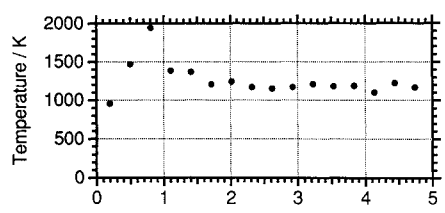

Fig. 11a Rotational temperature measured at nozzle station N1.

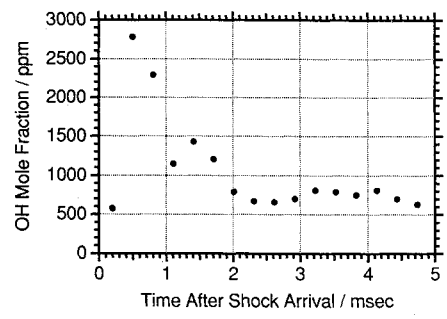

Fig. 11b OH mole fraction measured at nozzle station N1.

Analyzing the data in Fig. 4 for OH mole fraction generates the data shown in Fig. 11b. This plot of OH mole fraction vs time after shock arrival displays data recorded during the measured test time. The first several points in the figure are the equivalent OH mole fraction associated with the tail end of the nozzle flow establishment period and are to be disregarded for reasons mentioned earlier. It is shown to illustrate how OH mole fraction plots can also be used to measure the extent of the clean test period. OH mole fraction is measured at an average value of 725 ppm with ±10% variation over the test period, and clearly fluctuates more than its time equivalent temperature. The distribution of water in the driven tube nitrogen was not as well understood as in the tests where the fixed wavelength technique was applied. This may be responsible for the increased fluctuations in absorption seen in the scanned wavelength data. Also, the variation in time between the scans of the two rotational transitions may account for the mole fraction differences between the transitions as seen for some doublets.

Comparisons of this data with two-dimensional nonequilibrium computations of the 16-in. shock tunnel nozzle flow have been performed in coordination with Lee.[17] The agreement for temperature is excellent (less than 1%), whereas the computed mole fractions agree to within 50%. Although encouraging, these results require that further measurements be made to appropriately validate the chemical kinetic reaction mechanism and the model for molecular internal energy storage.

A similar application of OH absorption spectroscopy in shock tunnel flows has recently been conducted at the Calspan shock tunnel facility by Lempert[18,19] using a microwave discharge resonance light source. The lamp forms a plasma discharge dominated by H atoms and OH. Using this multiline source and mechanically chopping its output at 5 kHz, two narrow spectral regions are monitored providing sensitivity to both OH number density and temperature. The specific application at Calspan was in a scramjet combustor environment using uv transmitting optical fiber to transmit and collect the beam. The relatively low power of the microwave discharge source made discrimination of signal absorption by OH from emission of OH in the luminous environment of the combustor difficult. The very narrow linewidth of the cw laser absorption system coupled with its high energy output may make it a more appropriate diagnostic system to apply in combustor environments.

Conclusions

We have demonstrated the capability to operate the Ames 16-in. shock tunnel free of contamination that would otherwise limit proper application of laser-based flow diagnostics. The key lessons learned concern development of instrumentation and quantitative testing in a large impulse facility. It was clearly established that emission spectroscopy must become a routine diagnostic used in conjunction with the laser system to help identify and eliminate sources of flow contamination unique to high-enthalpy shock tunnel flows. Further enhancement of the spectroscopic capability will also allow measurement by emission or absorption spectroscopy of species important to high-enthalpy flow physics that are not, at the present, accessible by laser light sources.

We applied a high-sensitivity uv laser absorption instrument to expanding nozzle flows in the shock tunnel facility nozzle allowing time-resolved species mole fraction and temperature measurements at sample frequencies of 3.3 kHz. Operating in either the fixed frequency or the rapid wavelength scanning mode, the test time was shown to be approximately 3–5 ms for the conditions tested. This significantly exceeds the test times normally associated with pulsed facilities. The OH mole fraction and temperature measurements have provided some of the first quantitative experimental data in high-enthalpy, hypersonic expanding flows for comparison with thermal and chemical nonequilibrium flow codes. The high-frequency wavelength scanning capability also allows measurement of broadened rotational line profiles providing the potential for determination of flow velocity and pressure.[20,21] In long turnaround time, short test time impulse facilities, data must be maximized. Therefore, multiple position absorption paths through the flow can be monitored with fiber optic beam transfer,[22] and multidimensional diagnostic instrumentation must be applied where extensive optical access is possible.[7] Finally, continued development of advanced computational tools must proceed in concert with experiments to interpret data, validate the codes, and help direct future research.

Acknowledgments

The authors thank the following people for their contributions to this research effort and for their continuing support: Ronald Hanson and his research assistants Albert Chang and Michael DiRosa of the High Temperature Gasdynamics Laboratory at Stanford University for their outstanding support in the initial application development stage and for their continued consultation; David Bogdanoff, Horacio Zambrana, and Tim Tam of the Aerothermodynamics Branch for their expert assistance in areas of shock tunnel processes, data acquisition, and optical applications; and Robert Miller, Charles Cornelison, and Warren Norman of the Thermophysics Facilities Branch and Donald Holt, Daniel Theroux, Donald Bowling, and Michael Phillips of Arvin/Calspan Corporation for their technical support in shock tunnel operations.

References

[1]Bogdanoff, D. W., Zambrana, H. A., Cavolowsky, J. A., Newfield, M. E., Miller, R. J., and Cornelison, C., "Reactivation and Upgrade of the NASA Ames 16-Inch Shock Tunnel: Status Report," AIAA 30th Aerospace Sciences Meeting, AIAA Paper 92-0327, Reno, NV, Jan. 1992.

[2]Cavolowsky, J. A., Bogdanoff, D. W., and Hanson, R. K., "Test and Diagnostic Capability for High Mach Number Propulsion Testing in the Ames Pulse Facility (Unclassified)," Tenth NASP Symposium, Paper 254, Monterey, CA, April 1991.

[3]Bogdanoff, D. W., Cavolowsky, J. A., Park, C., and Deiwert, G. S., "Ames 16-Inch Shock Tunnel Performance Characteristics and Diagnostic Capabilities for High Speed Combustors (Unclassified)," Ninth NASP Symposium, Paper 112, Naval Training Center, Orlando, FL, Nov. 1990.

[4]Bogdanoff, D. W., Deiwert, G. S., Strawa, A. W., and Cavolowsky, J. A., "Ames Shock Tunnel Facility Calibration and Initial Test Results (Unclassified)," Seventh NASP Symposium, Paper 80, NASA Lewis Research Center, Cleveland, OH, Oct. 1989.

[5]Cavolowsky, J. A., Bogdanoff, D. W., Hanson, R. K., Chang, A. Y., and DiRosa, M. D., "Laser Absorption Measurement of OH in Shock Tunnel Flows (Unclassified)," Seventh NASP Symposium, Paper 78, NASA Lewis Research Center, Cleveland, OH, Oct. 1989.

[6]Strawa, A. W., and Cavolowsky, J. A., "Development of Non-Intrusive Instrumentation for NASA Ames' Ballistic Range and Shock Tunnel," AIAA 28th Aerospace Sciences Meeting, AIAA Paper 90-0628, Reno, NV, Jan. 1990.

[7]Hanson, R. K., Chang, A. Y., DiRosa, M. D., Philippe, L. C., McMillin, B. K., and Lee, M. P., "Laser-Based Diagnostics for Propulsion and Hypersonics Testing," AIAA 16th Aerodynamic Ground Testing Conference, AIAA Paper 90-1383, Seattle, WA, June 1990.

[8]Cavolowsky, J. A., Newfield, M. E., Tam, T. C., Loomis, M. P., Bogdanoff, D. W., and Zambrana, H. A., "Flow Characterization in the NASA Ames 16-Inch Shock Tunnel," 28th AIAA/SAE/ASME/ASEE Joint Propulsion Conference, AIAA Paper 92-3810, Nashville, TN, July 1992.

[9]Rea, E. C., Jr., Salimian, S., and Hanson, R. K., "Rapid-Tuning Frequency-Doubled Ring Dye Laser for High Resolution Absorption Spectroscopy in Shock Heated Gases," *Applied Optics,* Vol. 23, No. 11, 1984, pp. 1691–1694.

[10]Chang, A. Y., Rea, E. C., Jr., and Hanson, R. K., "Temperature Measurements in Shock Tubes Using a Laser-Based Absorption Technique," *Applied Optics,* Vol. 26, No. 5, 1987, pp. 885–891.

[11]Johanson, W., and Zambrana, H., "Using a Graphical Programming Language to Write CAMAC/GPIB Instrument Drivers," ISA Paper 90-067, 37th International Instrumentation Symposium, San Diego, CA, May 5–9, 1991.

[12]Rea, E. C., Jr., "Rapid Tuning Laser Wavelength Modulation

Spectroscopy With Applications in Combustion Diagnostics and OH Line Shape Studies," High Temperature Gasdynamics Lab. Rept. HTGL T-272, Stanford Univ., Stanford, CA, March 1991.

[13]Goldman, A., and Gillis, J. R., "Spectral Line Parameters for the $A^2\Sigma - X^2\Pi$ (0,0) Band for OH Atmospheric and High Temperatures," *Journal of Quantitative Spectroscopy and Radiative Transfer,* Vol. 25, No. 2, 1981, pp. 111–135.

[14]Drayson, S. R., "Rapid Computation of the Voigt Profile," *Journal of Quantitative Spectroscopy and Radiative Transfer,* Vol. 16, No. 7, 1976, pp. 611–614.

[15]Rea, E. C., Jr., Chang, A. Y., and Hanson, R. K., "Shock-Tube Study of Pressure Broadening of the $A^2\Sigma - X^2\Pi$ (0,0) Band of OH by Ar and N_2," *Journal of Quantitative Spectroscopy and Radiative Transfer,* Vol. 37, No. 2, 1987, pp. 117–127.

[16]Cambier, J.-L., Private communications, NASA Ames Research Center, Moffett Field, CA, Sept. 1991.

[17]Lee, S.-H., Bogdanoff, D. W., Cavolowsky, J. A., and Park, C., "Nonequilibrium H_2-Air Reactions in Shock Tunnel Nozzle," AIAA/ASME Fifth Joint Thermophysics and Heat Transfer Conference, AIAA Paper 90-1751, Seattle, WA, June 18–20, 1990.

[18]Lempert, W. R., "Microwave Resonance Lamp Absorption Technique for Measuring Temperature and OH Number Density in Connbustion Environments," *Combustion and Flame,* Vol. 73, No. 1, 1988, pp. 89–98.

[19]Orth, R. C., Torillo, D., Rizkalla, O. F., Lempert, W., and Erdos, J. I., "Results of the Parametric Scramjet Combustor Experiments Conducted in the Calspan Shock Tunnel—4th Entry," General Applied Sciences Lab., GASL TR 329, Ronkonkoma, NY, Feb. 1991.

[20]Davidson, D. F., Chang, A. Y., DiRosa, M. D., and Hanson, R. K., "Continuous Wave Laser Absorption Techniques for Gasdynamic Measurements in Supersonic Flows," *Applied Optics,* Vol. 10, No. 18, 1991, pp. 2598–2608.

[21]Chang, A. Y., Battles, B. E., and Hanson, R. K., "Simultaneous Measurements of Velocity, Temperature, and Pressure Using Rapid CW Wavelength-Modulation Laser-Induced Fluorescence of OH," *Optics Letters,* Vol. 15, No. 12, 1990, pp. 706–708.

[22]Hanson, R. K., Salimian, S., Kychakoff, G., and Booman, R. A., "Shock-Tube Absorption Measurements of OH Using a Remotely Located Dye Laser," *Applied Optics,* Vol. 11, No. 5, 1981, pp. 641–643.